JEE Journal of Ecological Engineering

Journal of Ecological Engineering, 2025, 26(1), 83–94
https://doi.org/10.12911/22998993/195264
ISSN 2299–8993, License CC-BY 4.0

Received: 2024.10.21
Accepted: 2024.11.15
Published: 2024.12.01

Monitoring and assessment of sand encroachment near Sakala solar farm – Results from field observations

Nejib Ghazouani[1], Mohamed Taieb Labiadh[2], Yahya Alassaf[1], Atef Rezgui[3], Sivaguru Rajendran[4]

[1] Department of Civil Engineering, College of Engineering, Northern Border University, Arar, 73222, Saudi Arabia
[2] Institute of Arid Regions of Medenine, 4119 Medenine, Tunisia
[3] AH Environmental Consulting, Khobar, Saudi Arabia
[4] Al Jomaih Energy and Water (JENWA), Saudi Arabia
* Corresponding author's e-mail: nejib.ghazouani@nbu.edu.sa

ABSTRACT

This study investigated wind erosion and soil particle distribution at the Sakaka Solar Power Plant in Saudi Arabia, assessing the potential impacts on solar panel efficiency and site management. Soil samples from various locations within the site were analyzed using a sieve-based approach and log-normal function fitting to characterize particle size distributions. The analysis revealed two consistent size modes across all samples: a primary mode centered around 524 μm and a secondary mode at approximately 168 μm, with an additional fine sand population around 100 μm. Wind erosion and soiling events were monitored using big spring number eight (BSNE) sediment samplers strategically placed around the site. Results showed significant spatial and temporal variations in sediment fluxes, with the highest rates observed in the West (149.05 kg/m), Southwest (47.14 kg/m), and Northwest (9.42 kg/m) sectors. The total drift during the study period was 205.61 kg/m, with 66% of the annual total occurring between May and August, aligning with the region's known wind patterns. Detailed analysis of erosion events revealed that the western quadrant of the site consistently experienced the highest erosion fluxes, up to 13 times greater than those in the southern quadrant during peak events. The effectiveness of existing erosion control measures, such as a sand ridge 180 meters upwind of the western boundary, was found to be limited, reducing sand flux by only 58% at the nearest monitoring station. These findings highlight the critical need for targeted erosion mitigation strategies, particularly along the western perimeter of the solar plant. The study underscores the importance of considering soil texture and local wind patterns in the assessment and management of wind erosion risks at solar power installations in arid environments.

Keywords: aeolian processes, PV power plants, wind erosion, exponential decay, horizontal flux.

INTRODUCTION

The global energy landscape is undergoing significant transformation, with renewable energy sources, particularly solar power, playing an increasingly prominent role. This shift is driven by the urgent need to address climate change, reduce greenhouse gas emissions, and ensure energy security (REN21, 2023). Saudi Arabia, traditionally known for its oil-based economy, has embarked on an ambitious energy transformation plan as part of its Vision 2030 initiative (VAR23, 2023). This plan aims to diversify the country's energy mix and reduce its dependence on fossil fuels by significantly increasing the share of renewable energy in its power generation portfolio (IRENA, 2023). The Sakaka Solar Power Plant, with a capacity of 300 MW, represents a cornerstone of this transformation, marking Saudi Arabia's first utility-scale solar project (ACWA Power, n.d.; Imam et al., 2024). However, the deployment of large-scale solar facilities in arid regions like Saudi Arabia presents unique challenges that require careful consideration and innovative solutions.

While arid regions often offer abundant solar resources, they also present severe environmental

conditions that can impact the performance and longevity of solar energy facilities. Two primary challenges in these environments are sand encroachment and dust soiling. In desert environments, the movement of sand dunes and the transport of sand particles by wind pose significant risks to solar installations. Sand encroachment can lead to physical damage to solar panels, abrasion of protective surfaces, and even structural instability of mounting systems (Labiadh et al., 2024; Yao et al., 2022). The dynamic nature of sand movement in these regions necessitates a thorough understanding of local aeolian processes and implementation of effective mitigation strategies.

Dust soiling is the second challenge for large-scale solar plants. In recent studies investigating the impact of dust accumulation on photovoltaic (PV) module performance, researchers have employed experimental methodologies under both controlled and real-world conditions. A study focusing on monocrystalline and polycrystalline PV modules found that a dust density of 4.6 g/m² led to output power reductions of 16% and 11%, respectively (Majeed et al., 2020). Similarly, research conducted in a Saharan environment revealed that after 8 weeks of outdoor exposure, 4.36 g/m² of dust accumulation resulted in an 8.41% drop in maximum power output, with a single sandstorm causing a 32% reduction in energy generation for a 30 MW grid-connected PV power plant (Dida et al., 2020). The composition, size distribution, and deposition rates of dust particles vary significantly across different arid regions, making site-specific studies crucial for developing effective cleaning and maintenance protocols. A study on dust deposition effects on solar panels under desert conditions found that dust particles ranged from 0.4 μm to 31 μm in size. As dust density increased 3.3 times from 0.001 g/cm^2, photovoltaic normalized maximum power decreased by 98.13% (Sadat et al., 2021). Under similar conditions to Saudia Arabia, a study on a large-scale 2 GW photovoltaic (PV) plant revealed significant seasonal variations in energy production, with annual generation ranging from 2.96 to 3.11 million MWh (Alshawaf et al., 2020). Notably, the study observed that solar variability in winter was twice that of demand variability, and prolonged sandstorms (12 hours or more) could reduce daily solar irradiance by up to 60%.

Over the last decade, a much research work was devoted to PV monitoring programs of dust accumulation and aeolian sand transport and highlighted the importance of monitoring dust accumulation and cleaning the panels regularly to maintain their performance (Said et al., 2024; Zhao et al., 2021). The authors have proposed different monitoring techniques for detecting dust accumulation on PV panels, including using cameras and imaging sensors, measuring changes in current-voltage characteristics, and analyzing the spectral reflectance of the panels. These monitoring techniques can provide real-time data on the amount and type of dust accumulation on PV panels, enabling prompt cleaning and maintenance. Nevertheless, they often rely on complex, expensive instrumentation that can be challenging to deploy and maintain in remote or harsh environments.

While the techniques above are being increasingly used, standard techniques using aeolian sand sampling methods are still in place due to their relative accuracy and reliability. For instance, the big spring number eight (BSNE) sampler offers a cost-effective and efficient alternative for monitoring aeolian sediment transport and dust deposition and still widely used in such research purposes (Meng et al., 2024; Ren et al., 2024; Vickery and Eckardt, 2021). This passive sampling device requires no power source, has no moving parts, and can be easily installed and maintained in harsh environments. BSNE samplers enable extended deployment periods and facilitate comprehensive spatial and temporal dust monitoring without the need for sophisticated equipment. This approach reduces financial barriers and contributes to a better understanding of dust dynamics and their impacts on solar energy systems and the environment.

A quick bibliometric analysis for the last four year reveals numerous studies having investigated the impacts of dust soiling and soil aeolian transport on solar panels in arid environments in China (Tang et al., 2021; Wang et al., 2021; Wang et al., 2024), while scarce research work was identified on other geographic locations with similar challenges (Al-Dousari et al., 2020; Labiadh et al., 2023). The reason for extensive research work in China, less observed in other countries, may be explained by the proliferation of power energy facilities which enables the researcher to conduct case-based investigation. In Saudi Arabia, the first utility-scale solar power plant has been constructed very recently near Sakaka city. To the best of authors knowledge, the present study is the first case-based investigation of wind-induced sediment transport conducted at

an operating power plant and aimed to contribute in bridging the notable gap in the literature regarding the comprehensive characterization of soil particle distributions and their relationship to wind erosion patterns, specifically in the context of large-scale solar installations in Saudi Arabia.

The current research aimed to bridge this knowledge gap by:

1. Analyzing the particle size distribution of soil samples from various locations within the Sakaka Solar Power Plant site.
2. Quantifying wind erosion rates and patterns using strategically placed sediment samplers.
3. Evaluating the effectiveness of existing erosion control measures.
4. Providing insights into the spatial and temporal variations of erosion risks across the site.

To achieve these objectives, the study employed a multi-faceted approach combining field measurements, laboratory analysis, and statistical modeling:

- particle size analysis – soil samples were analyzed using a sieve-based method, with the resulting data fitted to log-normal distributions. This approach allows for the characterization of distinct particle size modes and their relative contributions to the overall soil composition.
- wind erosion monitoring – BSNE sediment samplers were deployed across the site to capture wind-blown particles. This method provides quantitative data on sediment fluxes and their spatial variability.
- temporal analysis – the study examined seasonal variations in erosion rates, particularly focusing on the summer months (May to August) when wind activity is typically highest in the region.
- spatial pattern analysis – by comparing sediment fluxes at different locations within the site, the research aimed to identify the areas of high erosion risk and evaluate the effectiveness of existing protective measures.

The findings of this study have significant implications for the design, operation, and maintenance of solar energy facilities in arid environments. By providing a detailed characterization of soil properties and erosion patterns specific to the Sakaka site, the research contributes to the development of more effective erosion control strategies and maintenance protocols. Furthermore, the methodologies employed in this study can serve as a template for similar assessments at other solar installations in development and commissioning phases similar various several geographical and climatic contexts in Saudi Arabia. As the global deployment of solar energy continues to accelerate, particularly in desert environments, such site-specific studies will be crucial for optimizing the performance and ensuring the long-term sustainability of these facilities.

In conclusion, this research bridged a critical knowledge gap in the local deployment of large-scale solar energy facilities in arid environments in Saudi Arabia and similarly climatic environments. By providing detailed insights into the soil characteristics and erosion dynamics at the Sakaka Solar Power Plant, this study delivered critical field-based evidence of sediment transport patterns and rates, bridging a knowledge gap in the design and optimization of sand mitigation measures for utility-scale solar facilities in desert environments.

MATERIALS AND METHODS

Study area

The research was conducted in the periphery of the Sakaka solar farm, located in the Al Jouf region of Saudi Arabia (Figure 1). The solar park has an installed capacity of 405 MWp and spans an area of approximately 6.3 km². The facility is situated on a perfectly flat terrain. The solar farm comprises photovoltaic (PV) modules mounted on structures, inverter stations, and is enclosed by a 10 km long security fence. During the construction phase of the solar park, significant quantities of construction solid waste (CSW). This waste consisted of sand, stones, and rock debris resulting from full mass and trench excavation work. CSW was deposited randomly in stockpiles around the close vicinity of the plant, particularly along portions of the west, south, and east boundaries. The southern and western boundaries were notably affected, with large quantities of sand dumped within the plant berms. These deposits altered the local topography and increased the susceptibility of the area to wind erosion as well as sand encroachment.

To mitigate sand encroachment, artificial sand ridges (counter dunes) are being installed perpendicular to the prevailing westerly winds. This common protective measure for desert installations spans 2050 m along the site's western boundary, with 50 m extensions at right angles on

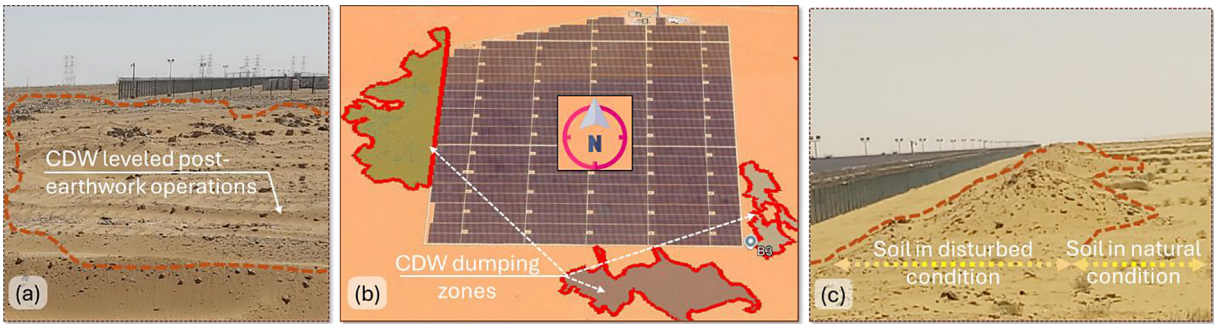

Figure 1. Sakaka solar farm and surrounding area (a) Photo taken from the West towards the NW fence corner (b) Aerial view of the Sakaka solar farm and surrounding area, captured in February 2021 (Source: Google Earth ©), (c) Southern border: Ground-level photograph illustrating the contrast between disturbed and undisturbed soil surfaces at the study site

the Northwest and Southwest ends. The trapezoidal ridges are positioned 30–50 m from the solar plant's fence line. A top each ridge, a 120 cm porous fence will be installed, with 40 cm anchored in the sand. These fences will be constructed using local materials such as palm leaves, plant boughs, or manufactured materials like corrugated cement or metal plates, or plastic fillets (Figure 2). The interim sand mitigation system comprises a counter dune structure fabricated from excavation-derived CDW. While this provisional measure provides basic protection against probable

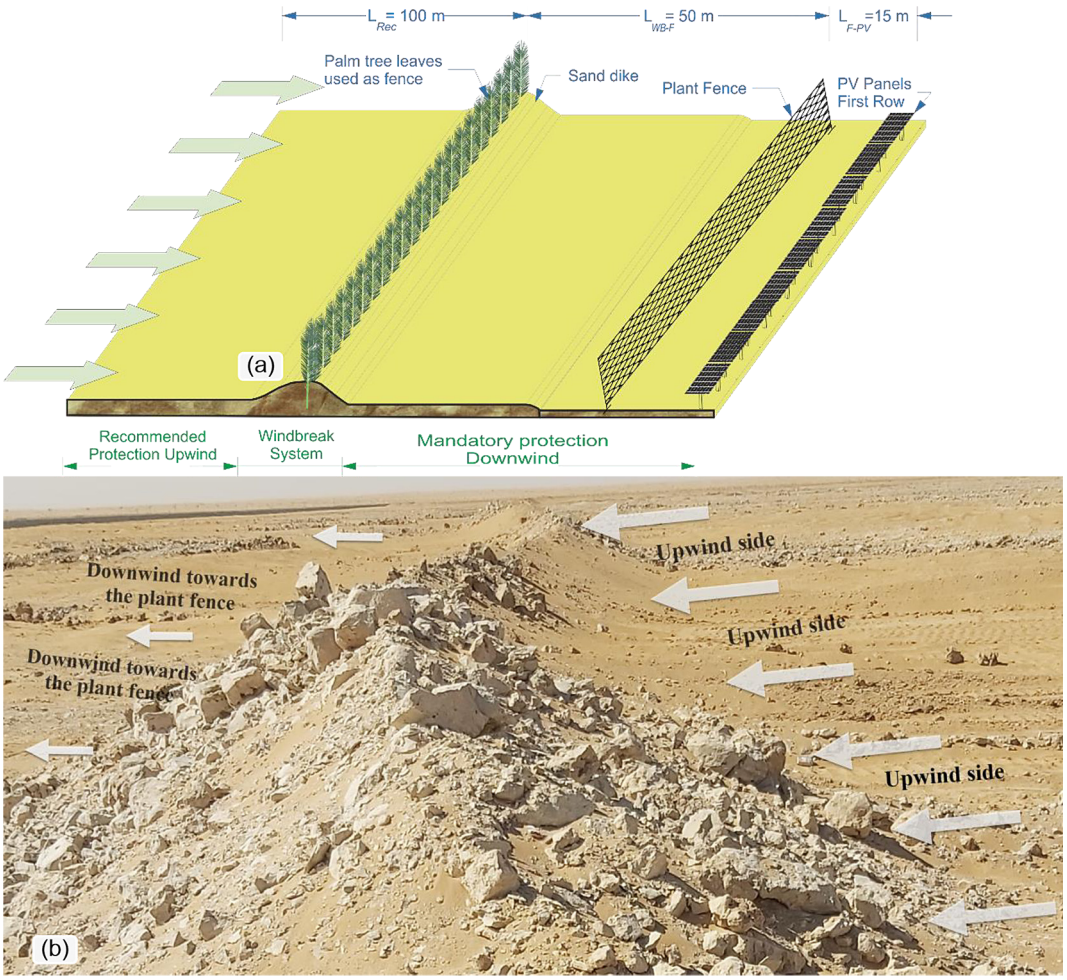

Figure 2. Mechanical SMM consisted of artificial sand ridge: (a) layout with annotation of key components, (b) photo from construction site showing SMM earthmoving work in progress

operational disruptions caused by aeolian sediment transport, the permanent design will be optimized using the data from ongoing quantitative assessments of windblown sediment dynamics.

Historical weather data analysis

To determine the episodes of soiling and erosion, a comprehensive analysis of historical meteorological data was conducted. Data spanning 20 years (1999–2018) were obtained from a weather station located approximately 6 km from the Sakaka solar farm. The data included continuous measurements of wind speed and direction, air temperature, relative humidity, and rainfall. Statistical processing of the weather data series was performed to derive key parameters influencing wind erosion processes. The analysis focused on identifying wind regimes, prevailing wind directions, and periods with wind speeds exceeding the threshold required to initiate soil particle movement. Wind rose diagrams and frequency distributions were generated to visualize wind patterns, which were critical for designing the layout of soil samplers around the solar plant.

Soil grain size analysis

Sieve analysis was conducted according to standard test methods for particle-size distribution (gradation) of soils using sieve analysis (ASTM D6913/D6913M-17). The samples were collected during the field campaign: one from within the solar plant and two from outside the fence line (west and south boundaries). Each sample consisted of soil collected from various locations of the selected area to ensure representativeness. Understanding the soil grain size distribution is critical, as it influences both the threshold wind velocity required for particle movement and the rate of soil transport.

Field measurements of soil fluxes – the horizontal soil flux was measured using BSNE samplers, known for their efficiency in collecting wind-transported sediments (Figure 3).

The BSNE samplers feature extended mouths aligned into the wind by a vane, allowing airborne particles to enter the collection chamber while the wind exits through a fine steel mesh. This design enables the sampling of materials to move near the soil surface at different heights.

Figure 3b shows three vertically aligned sediment catchers mounted on a pole at different heights. An operator is seen conducting a functionality check by holding a tissue paper strip near the samplers, visually confirming proper airflow essential for accurate sediment collection during wind erosion events. The field measurements were conducted between July 21st, 2020, and August 5th, 2020. To capture wind erosion fluxes event by event, the layout of the BSNE samplers was optimized based on prevailing wind directions identified from historical data. Given the extent of the area affected by delta oiling effects, particularly along the west and south borders (up to approximately 800 m), it was determined that the samplers should be installed at the edges of the west and south fence lines of the solar plant (Figure 2). This placement ensured that the samplers were within the stabilized saltation layer where soil particle movement is most significant.

A total of five stations, labeled A through E, were established, each equipped with a pole supporting three BSNE samplers at varying heights to capture vertical profiles of sediment flux. The installation heights ranged from approximately 10.5 cm to 66 cm above ground, which is appropriate given that the saltation layer under natural conditions typically extends to less than 1 meter.

Computational analysis of horizontal flux

Wind erosion is a complex process involving the detachment, transport, and deposition of soil particles by wind action. Accurate measurement and modeling of wind erosion fluxes are essential for understanding sediment transport dynamics and for developing effective soil conservation strategies. BSNE samplers are used to measure wind erosion fluxes at different heights. The heights were measured at the time of installation and re-measured after each erosion event to account for any changes in ground level due to sediment deposition or erosion. Measurements were taken along the axis of the prevailing wind direction to capture any topographical variations influencing the flux. Following each wind erosion event, the sediment collected in the BSNE samplers was retrieved and weighed. The horizontal mass flux $q(z)$ at each sampling height was calculated using (Ma et al., 2010):

$$q(z) = \frac{m(z)}{A(z).t} \quad (1)$$

where: m – mass of trapped soil (g), A – inlet area of the BSNE sampler (cm^2), t – duration of the sampling period (s), z – height of the sampler above the ground (cm).

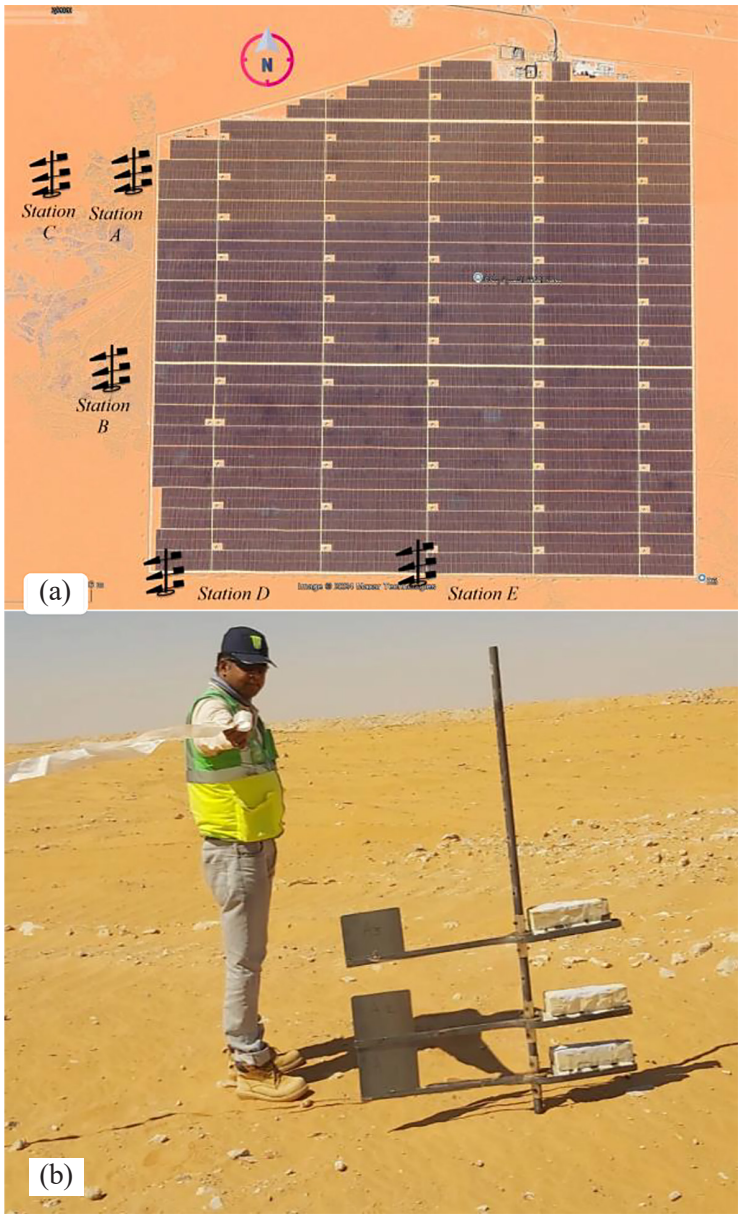

Figure 3. Soil flux measurement setup at Sakala solar farm (a) aerial view (Google Earth©) showing the considered layout of BSNE sampling stations around the solar farm perimeter. Stations A-E are marked, illustrating the comprehensive coverage of potential sand encroachment areas, (b) close-up of Station A, demonstrating the BSNE sampler configuration

The horizontal mass flux of wind-eroded particles decreases exponentially with height above the soil surface. This approach offers high-resolution data on sediment transport during specific wind events, which is valuable for understanding erosion processes and for developing targeted soil conservation measures.

The exponential decay function employed to model the horizontal flux of soil particles with height reads (Bauer and Davidson-Arnott, 2014; Ellis et al., 2009; Poortinga et al., 2014):

$$q(z) = a_1 e^{-a_2 z} \quad (2)$$

where: $q(z)$ – horizontal mass flux at height z (in g·cm^{-2}·s^{-1}); $a1$, $a2$ – adjustment coefficients (with units g^{-1} and g·cm^{-2}, respectively) determined through least squares regression; z – height above the soil surface (in cm).

The integration of this function over the measured height range allowed for the estimation of the total horizontal soil flux (Q):

$$Q = \int_{z_1}^{z_2} q(z)dz = \left[-\frac{a_1}{a_2} e^{-a_2 z}\right]_{z_1}^{z_2} \quad (3)$$

where: z_1 and z_2 represent the minimum and maximum sample heights, respectively.

Some comments on the exponential decay function include:

- a_1 – represents the horizontal flux at the soil surface (z = 0). It indicates the maximum flux,
- a_2 – describes the rate of decay of the flux with height. A larger a_{12} means a rapid decrease in flux with height,
- near the soil surface, particle concentrations are highest due to direct training,
- as height increases, the concentration of particles decreases exponentially because:
  - heavier particles (saltation and creep) cannot be lifted to higher altitudes.
  - finer particles (suspension) can reach higher altitudes but are present in lower concentrations.

Major wind erosion episodes

Wind erosion events were selected for soil flux measurements based on wind speed and direction data, ensuring that the conditions were conducive to soil movement from specified directions relative to the solar plant. Three significant erosion events were identified during the monitoring campaign using the available online weather forecasting sites (Weather Maps, Live Satellite and Weather Radar, n.d.; Windfinder.com, n.d.):

- Event 1 – occurred on July 21st, 2020, with a maximum wind speed of 6.4 m/s from the northwesterly quadrant.
- Event 2 – occurred on July 26th, 2020, with a maximum wind speed of 5 m/s from the southwesterly quadrant.
- Event 3 – spanned from August 1st to August 5th, 2020, characterized by daytime wind erosion with intermittent pauses in the evenings. The maximum recorded wind speed during this period was 7.1 m/s, primarily from the west (270°).

RESULTS AND DISCUSSION

Weather data analysis

The statistical analysis of data aimed to draw relevant findings on the likelihood of weather conditions to contribute to the erosion transport events: wind regimes, air humidity and temperature variation trends should provide insightful information regarding the soiling effect.

The prevailing wind direction at the Sakaka solar farm is Northwest (NW). This is evident from the highest percentage values across multiple speed classes for the NW direction, particularly in the 3.0–4.4 m/s range (8.77%). The wind distribution reveals light winds (0–3.0 m/s) common from all directions, moderate winds (3.0–5.6 m/s) most frequent from the NW, WNW, and E to SE sectors, and stronger winds (greater than 6.0 m/s) which are relatively rare but occur most often from the W to NW sectors. After NW, the next most significant wind directions are WNW, E, and ESE, all showing notable frequencies in the moderate wind speed ranges. The highest average wind speeds (3.5 m/s) are observed from the ESE, W, WNW, and NW directions (Figure 4).

The temperature profile is characterized by a mean temperature of 23.15 °C, reflecting a generally warm climate, wide temperature range (SD 9.04 °C) indicating significant seasonal variations, slightly left-skewed, suggesting a tendency towards cooler temperatures, platykurtic distribution points to more frequent temperature extremes (Figure 5).

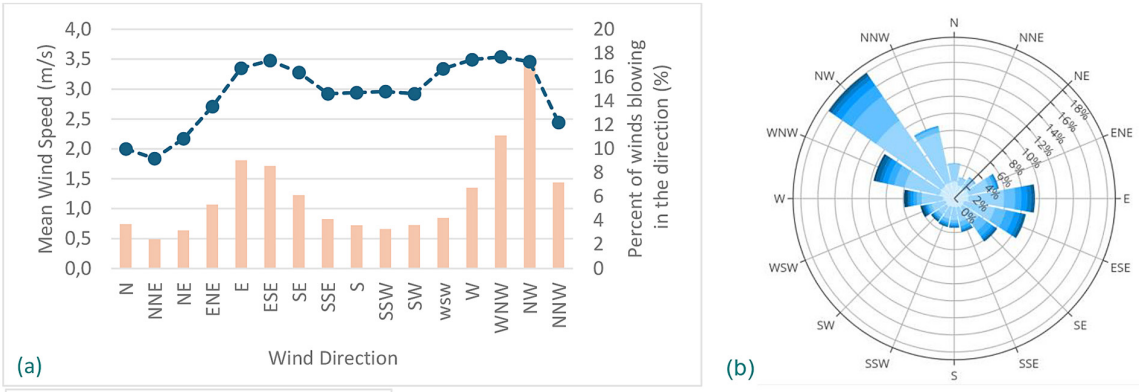

Figure 4. Wind speed analysis at Sakaka solar farm (a) wind direction and mean (b) windrose

The relative humidity data for Sakaka solar farm reveals low average humidity: 29.4%, indicating a dry climate, high variability: SD of 17.0% suggests significant fluctuations, right-skewed distribution (1.1): more frequent lower humidity with occasional higher values and slightly leptokurtic (0.43): slightly more peaked than normal distribution. This profile depicts an arid environment with occasional periods of higher humidity, typical of a desert climate with potential seasonal moisture variations (Figure 6).

In conclusion, the climate profile presents a challenging environment for the solar farm, characterized by warm temperatures with considerable fluctuations, moderate winds prone to occasional intensification, and predominantly dry conditions. These conditions likely influence sand movement patterns and solar panel efficiency, necessitating careful management strategies to optimize performance and mitigate the potential sand encroachment issues.

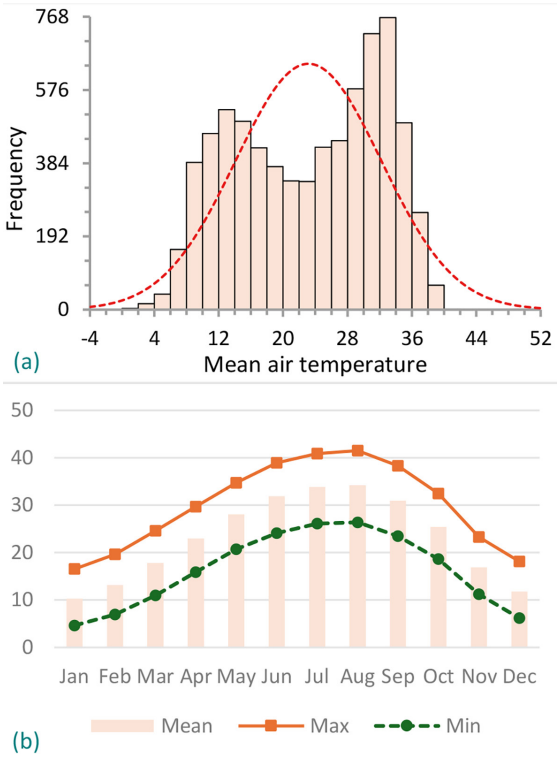

Figure 5. Air temperature analysis at Sakaka solar farm (a) frequency distribution of mean air temperatures (b) seasonal variation of air temperature (minimum, maximum, and mean)

Soil grain size

Sieve analysis was conducted on three soil samples (Western Sample-WS, Southern Sample-SS, Middle Sample-MS) from the Sakaka Solar Farm site. Figure 7 presents the particle size distribution curves. All samples showed predominantly sandy composition, with varying proportions of fines (silt and clay). The WS and SS exhibited similar gradation characteristics, while MS displayed distinct differences. WS and SS samples depicts peak retention observed in medium sand range (0.5–0.25 mm), well-graded distribution, and lower fines content (< 10% passing #200 sieve). However, MS sample reveals more uniform distribution across size ranges, higher fines content (> 25% passing #200 sieve), and poor gradation compared to WS and SS.

A fitting procedure was employed as further statistical processing of sieve analysis data and to estimate the key statistical parameters (m and σ). For the samples in this study, a two-mode approach (i.e., two log-normal functions) was determined to be optimal based on predefined threshold values for the minimization test.

The analysis yielded two consistent size modes across all samples collected from various locations within the site (Table 1). The primary mode, generally dominant, centered around 524 µm, while a secondary mode was observed at approximately 168 µm.

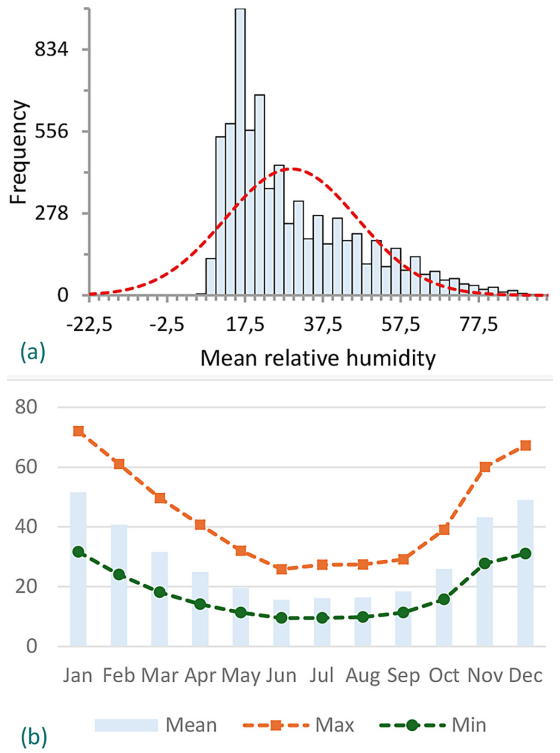

Figure 6. Air temperature analysis at Sakaka solar farm (a) frequency distribution of mean air temperatures (b) seasonal variation of air temperature (minimum, maximum, and mean)

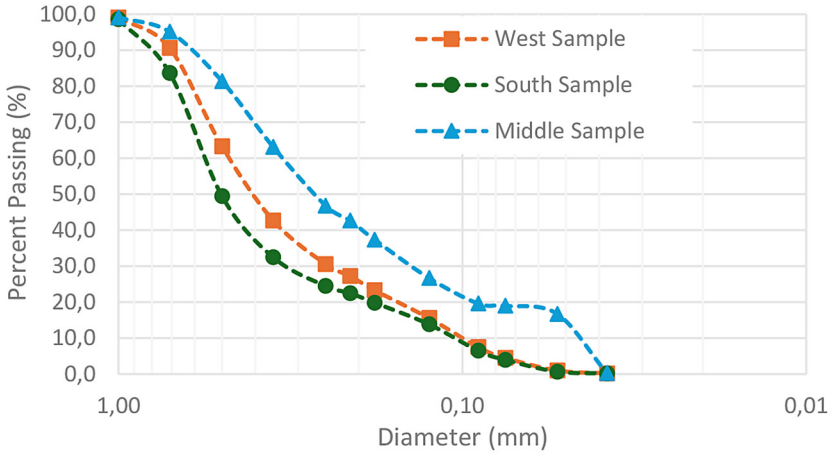

Figure 7. Grain size distribution of the samples collected at three locations of the study area

Table 1. Characteristics of mass size distribution modes for soil samples

Location	Sample collected inside the site		Sample from the west boundary		Sample from the south boundary	
Mode	Mode 1	Mode 2	Mode 1	Mode 2	Mode 1	Mode 2
PI (MM)	65%	35%	49.6%	50.4%	62.9%	37.1%
Std	1.48	1.53	1.30	2.12	1.28	2.08
Median (μm)	424	147	548.9	195.3	598.4	169.4

The primary mode, with median diameters ranging from 424 to 598.4 μm, suggests the presence of coarser aggregates at the soil surface. This coarser fraction could potentially increase the wind erosion threshold, thereby reducing the erodibility of these surfaces. The secondary mode, characterized by median diameters between 147 and 195.3 μm, represents an intermediate population contributing 35% to 50.4% of the total mass.

Of note is the presence of a fine sand population, with diameters approximating 100 μm. This size fraction is significant, as it corresponds to the grain size range requiring minimum wind energy to initiate aeolian erosion. The consistent observation of this population across samples indicates a high potential for wind erosion in most soils at the site.

The particle size distribution analysis of the Sakaka solar plant soils has revealed essential commonalities and differences in erodible soil grain-size distributions. The quasi-systematic presence of a coarser mode (median ~524 μm) may provide some resistance to erosion. However, the significant contribution of finer modes, particularly the presence of easily erodible fine sand, suggests that most soils in this site have the potential to be readily eroded by wind. These findings underscore the importance of considering soil texture in the assessment and management of wind erosion risks at solar power installations in arid environments. Further research into the spatial variability of these distributions and their relationship to local wind patterns could provide valuable insights for erosion mitigation strategies.

Soil flux measurement results

After wind erosion and soiling events, soil and dust storm samples were collected and analyzed. The samples were carefully collected in plastic bags and weighed, each identified by a unique box number corresponding to its BSNE station (Figure 8).

The results of wind erosion and sediment flux computations are summarized (Table 2). The analysis revealed significant spatial and temporal variations. Indeed, the highest sediment fluxes were observed in the West (149.05 kg/m), Southwest (47.14 kg/m), and Northwest (9.42 kg/m) sectors, with a total drift of 205.61 kg/m. These patterns align with known wind characteristics in Saudi Arabia, where western and southern winds are typically strongest. Seasonal trends showed peak erosion from May to August, accounting for 66% of the annual total drift. Spatial analysis consistently identified the western quadrant (stations A, B, C) as the most susceptible to erosion.

Figure 8. Sediment samples collected from BSNE stations, sorted by erosion event

Table 2. Characteristics of mass size distribution modes for soil samples

Events (Wind direction)	Station A	Station B	Station C	Station D	Station E
7/21/2020 (NW)	0.18	4.34	0.97	2.29	1.64
7/26/2020 (SW)	0.04	0.52	0.06	0.33	0.05
08/01 through 05/2020 (W)	26.17	51.03	61.69	7.82	2.35

During the most intense event (August 1–5, 2020), erosion fluxes in the western quadrant were 13 times higher than in the southern quadrant (stations D, E). Similar patterns were observed in other events, such as those on July 21st and 26th. These findings, derived from BSNE measurements, confirm the sensitivity of the landscape to wind erosion processes and highlight the need for targeted mitigation strategies, particularly in the western sectors of the site.

Analysis of the data in Table 2 reveals important insights into the erosion patterns and effectiveness of mitigation measures. Station A, benefiting from a sand ridge 180 meters upwind, collected only 42% of the sand flux observed at Station C during the third event. This indicates that while the sand ridge provides some shelter, its current distance from the project fence limits its effectiveness as a protective measure. Station B, situated at the border between natural and disturbed zones, collected 83% of Station C sand flux, suggesting similar erosion vulnerability in both areas despite different land use. Notably, Station C, located at the western boundary, consistently collected the highest sand flux, comparable to Station B. This persistent high flux at Station C implies that the western boundary remains a significant source of sand drift hazard for the plant, even if sand waste is removed from the immediate vicinity. These findings underscore the need for more effective erosion control strategies, particularly along the western perimeter of the site.

CONCLUSIONS

This comprehensive study of wind erosion and soil particle distribution at the Sakaka Solar Power Plant in Saudi Arabia has yielded several significant findings and highlighted important considerations for solar energy deployment in arid environments. The key findings of the investigation include:

Soil particle distribution: The analysis revealed a consistent bimodal distribution of soil particles across the site, with a primary mode centered around 524 μm and a secondary mode at approximately 168 μm. The presence of a fine sand population (~ 100 μm) indicates a high susceptibility to wind erosion.

Spatial variation in erosion: The western, southwestern, and northwestern sectors of the site experienced the highest sediment fluxes, with rates of 149.05 kg/m, 47.14 kg/m, and 9.42 kg/m, respectively. This pattern aligns with the predominant wind directions in the region.

Temporal patterns: A significant seasonal trend was observed, with 66% of the annual total

drift occurring between May and August, coinciding with periods of increased wind activity.

Effectiveness of erosion control measures: The existing sand ridge, located 180 meters upwind of the western boundary, showed limited effectiveness, reducing sand flux by only 58% at the nearest monitoring station.

Persistent western boundary risk: Despite mitigation efforts, the western boundary remains a significant source of sand drift hazard, with erosion fluxes up to 13 times higher than in other areas during peak events.

These findings underscore the critical importance of site-specific assessments and tailored mitigation strategies for solar energy installations in desert environments. The persistent high erosion rates, particularly along the western perimeter, highlight the need for more robust and innovative protective measures.

Building upon the findings of this study, several key research directions emerge as promising avenues for further investigation:

Long-term monitoring: Establishing a continuous, long-term monitoring program would provide valuable insights into the evolution of erosion patterns over time and their correlation with climatic variables. This could involve the integration of automated sensors and remote sensing technologies for more comprehensive spatial and temporal coverage.

Advanced erosion control strategies: Future research should focus on developing and testing novel erosion control measures specifically designed for the conditions at Sakaka. This may include exploring advanced materials for sand barriers, optimizing the placement and design of protective structures, or investigating the potential of vegetation-based solutions adapted to arid environments.

Modeling and prediction: Developing predictive models that integrate local meteorological data, soil characteristics, and topography could enhance the ability to forecast erosion events and optimize maintenance schedules.

Economic impact analysis: A detailed assessment of the economic impacts of erosion and soiling on energy yield, equipment lifespan, and maintenance costs would provide valuable information for project planning and risk management in similar environments.

In conclusion, this study has provided crucial insights into the complex interplay between soil characteristics, wind patterns, and erosion dynamics at the Sakaka Solar Power Plant. These findings not only contribute to the optimization of this specific installation, but also offer valuable lessons for the broader deployment of solar energy in arid regions. As the global transition to renewable energy accelerates, such site-specific studies will play an increasingly important role in ensuring the efficiency, longevity, and sustainability of solar power installations in challenging environments. The research outlined above provides a roadmap for future investigations that can further enhance the understanding and management of these critical issues.

Acknowledgement

The authors gratefully acknowledge the approval and support of this research study by grant no. ENGA-2023-12-2384 from the Deanship of Scientific Research at Northern Border University, Arar, K.S.A.

REFERENCES

1. ACWA Power. (n.d.). *Sakaka PV IPP*. Retrieved October 20, 2024, from https://acwapower.com/en/projects/sakaka-pv-ipp/
2. Al-Dousari, A., Ramadan, A., Al-Qattan, A., Al-Ateeqi, S., Dashti, H., Ahmed, M., Al-Dousari, N., Al-Hashash, N., & Othman, A. (2020). Cost and effect of native vegetation change on aeolian sand, dust, microclimate and sustainable energy in Kuwait. *Journal of Taibah University for Science*, *14*(1), 628–639. https://doi.org/10.1080/16583655.2020.1761662
3. Ali Sadat, S., Faraji, J., Nazififard, M., & Ketabi, A. (2021). The experimental analysis of dust deposition effect on solar photovoltaic panels in Iran's desert environment. *Sustainable Energy Technologies and Assessments*, *47*, 101542. https://doi.org/10.1016/j.seta.2021.101542
4. Alshawaf, M., Poudineh, R., & Alhajeri, N. S. (2020). Solar PV in Kuwait: The effect of ambient temperature and sandstorms on output variability and uncertainty. *Renewable and Sustainable Energy Reviews*, *134*, 110346. https://doi.org/10.1016/j.rser.2020.110346
5. Bauer, B. O., & Davidson-Arnott, R. G. D. (2014). Aeolian particle flux profiles and transport unsteadiness. *Journal of Geophysical Research: Earth Surface*, *119*(7), 1542–1563. https://doi.org/10.1002/2014JF003128
6. Dida, M., Boughali, S., Bechki, D., & Bouguettaia, H. (2020). Output power loss of crystalline silicon photovoltaic modules due to dust accumulation

in Saharan environment. *Renewable and Sustainable Energy Reviews*, *124*, 109787. https://doi.org/10.1016/j.rser.2020.109787

7. Ellis, J. T., Li, B., Farrell, E. J., & Sherman, D. J. (2009). Protocols for characterizing aeolian mass-flux profiles. *Aeolian Research*, *1*(1), 19–26. https://doi.org/10.1016/j.aeolia.2009.02.001
8. Imam, A. A., Abusorrah, A., & Marzband, M. (2024). Potentials and opportunities of solar PV and wind energy sources in Saudi Arabia: Land suitability, techno-socio-economic feasibility, and future variability. *Results in Engineering*, *21*, 101785. https://doi.org/10.1016/j.rineng.2024.101785
9. IRENA. (2023). *World Energy Transitions Outlook 2023: 1.5°C Pathway*. International Renewable Energy Agency, Abu Dhabi. https://www.irena.org/-/media/Files/IRENA/Agency/Publication/2023/Jun/IRENA_World_energy_transitions_outlook_summary_2023.pdf?rev=bdaa6280cdef47dcb7bf5dfcfc75b88f
10. Labiadh, M. T., Ghazouani, N., Dhamane, S. R., Rezgui, A., AlKhoshi, Y., & Alassaf, Y. (2024). Towards a Quantification of Sand Accumulation Near Sakaka Solar Farm: Experimental Approach and Development of Mitigation Measures. In M. Ksibi, A. Negm, O. Hentati, A. Ghorbal, A. Sousa, J. Rodrigo-Comino, S. Panda, J. Lopes Velho, A. M. El-Kenawy, & N. Perilli (Eds.), *Recent Advances in Environmental Science from the Euro-Mediterranean and Surrounding Regions (3rd Edition)* (pp. 567–570). Springer Nature Switzerland. https://doi.org/10.1007/978-3-031-43922-3_128
11. Labiadh, M. T., Rajot, J. L., Sekrafi, S., Ltifi, M., Attoui, B., Tlili, A., Hlel, M., Bergametti, G., des Tureaux, T. H., & Bouet, C. (2023). Impact of Land Cover on Wind Erosion in Arid Regions: A Case Study in Southern Tunisia. *Land*, *12*(9), Article 9. https://doi.org/10.3390/land12091648
12. Ma R, Wang JH, Qu JJ, Liu J, Sun T, & Wei L. (2010). Study on protective effect of difference types of cotton haulm sand barriers. *Journal of Soil and Water Conservation*, *24*(2), 48–51.
13. Majeed, R., Waqas, A., Sami, H., Ali, M., & Shahzad, N. (2020). Experimental investigation of soiling losses and a novel cost-effective cleaning system for PV modules. *Solar Energy*, *201*, 298–306. https://doi.org/10.1016/j.solener.2020.03.014
14. Meng, B., Gao, C., Lv, S., Han, G., Li, Z., Li, J., Wu, Q., & Zhang, F. (2024). The effects of grazing and the meteorologic factors on wind-sand flux in the desert steppe. *Frontiers in Environmental Science*, *12*. https://doi.org/10.3389/fenvs.2024.1428828
15. Poortinga, A., Keijsers, J. G. S., Maroulis, J., & Visser, S. M. (2014). Measurement uncertainties in quantifying aeolian mass flux: Evidence from wind tunnel and field site data. *PeerJ*, *2*, e454. https://doi.org/10.7717/peerj.454
16. Ren, H., Gao, X., Zhao, Y., Lei, J., De Maeyer, P., & De Wulf, A. (2024). Strong-wind events control barchan dune migration. *Communications Earth & Environment*, *5*(1), 1–9. https://doi.org/10.1038/s43247-024-01444-1
17. REN21. (2023). *Renewables 2023 Global Status Report Collection*.
18. Said, S. Z., Islam, S. Z., Radzi, N. H., Wekesa, C. W., Altimania, M., & Uddin, J. (2024). Dust impact on solar PV performance: A critical review of optimal cleaning techniques for yield enhancement across varied environmental conditions. *Energy Reports*, *12*, 1121–1141. https://doi.org/10.1016/j.egyr.2024.06.024
19. Tang, G., Meng, Z., Gao, Y., & Dang, X. (2021). Impact of utility-scale solar photovoltaic array on the aeolian sediment transport in Hobq Desert, China. *Journal of Arid Land*, *13*(3), 274–289. https://doi.org/10.1007/s40333-021-0096-y
20. VAR23. (2023). *Vision 2030 Annual Report*. Vision realization Office. https://www.vision2030.gov.sa/en/annual-reports
21. Vickery, K., & Eckardt, F. (2021). A closer look at mineral aerosol emissions from the Makgadikgadi Pans, Botswana, using automated SEM-EDS (QEMSCAN®). *South African Geographical Journal*, *103*(1), 7–21. https://doi.org/10.1080/03736245.2020.1824805
22. Wang, C., Hill, R. L., Bu, C., Li, B., Yuan, F., Yang, Y., Yuan, S., Zhang, Z., Cao, Y., & Zhang, K. (2021). Evaluation of wind erosion control practices at a photovoltaic power station within a sandy area of northwest, China. *Land Degradation & Development*, *32*(4), 1854–1872. https://doi.org/10.1002/ldr.3839
23. Wang, T., Liu, B., Tan, L., Niu, Q., Shi, B., Zhang, K., & Li, Z. (2024). Aeolian transport within a large-scale concentrated solar power plant in the Gobi region. *Geomorphology*, *455*, 109186. https://doi.org/10.1016/j.geomorph.2024.109186
24. *Weather Maps | Live Satellite & Weather Radar*. (n.d.). Meteoblue. Retrieved October 20, 2024, from https://www.meteoblue.com/en/weather-maps
25. Windfinder.com. (n.d.). *Windfinder—Wind, wave & weather reports, forecasts & statistics worldwide*. Windfinder.Com. Retrieved October 20, 2024, from https://www.windfinder.com
26. Yao, Z., Xiao, J., Xie, X., Zhu, H., & Qu, J. (2022). Design of optimal sand fences around a desert solar park—A case study from Phase IV of the Mohammed bin Rashid Al Maktoum Solar Park. *Natural Hazards*, *113*(1), 673–697. https://doi.org/10.1007/s11069-022-05319-6
27. Zhao, W., Lv, Y., Wei, Z., Yan, W., & Zhou, Q. (2021). Review on dust deposition and cleaning methods for solar PV modules. *Journal of Renewable and Sustainable Energy*, *13*(3), 032701. https://doi.org/10.1063/5.0053866